JOURNAL OF MATERIALS SCIENCE 25 (1990) 3880–3885

# Dispersion characteristics of sol–gel derived $(Ba_{0.2}Pb_{0.8})TiO_3$ at various pH

KYUNG HAW JO, EUNG SOO KIM, KI HYUN YOON
*Department of Ceramic Engineering, Yonsei University, Seoul, Korea*

The sol–gel derived $(Ba_{0.2}Pb_{0.8})TiO_3$ powder was observed for suspension behaviour as a function of pH (pH 1 to 13). The dispersion has an isoelectric point (IEP) at pH 7, and better dispersion was found at lower and higher pH than at pH 7. The powder has a BET surface area of $2.3\,m^2\,g^{-1}$ at pH 7 and 97 to $105\,m^2\,g^{-1}$ at pH 1, 11 and 13. The sol–gel specimens derived from well dispersed suspensions with pH 11 and 13 showed a high relative density (95 to 98%).

## 1. Introduction

In the improvement of the electrical and mechanical properties of advanced electronic ceramics, the method of powder preparation and control of the sintering process are important. There are chemical powder preparation methods via a liquid phase, such as the sol–gel method, in which it is easy to control the properties of the powder product and prepare fine particles. The sol–gel method has some merits, such as high purity, homogeneity, stoichiometric composition and infinite flexibility [1, 2] using a variety of organic raw materials, and it has been studied by many researchers [3, 4]. Fine (Ba, Pb)$TiO_3$ powder was prepared with a high rate of reactivity and good homogeneity by the sol–gel method [5]. It is, however, necessary to reduce the agglomeration and to control the interaction between particles in suspension. The high rate of reactivity results in shortening the sintering cycle and developing stability against grain growth. Therefore research on suspension behaviour is necessary but this can proceed only at a finite pace [6, 7].

Basically there are two types of dispersion mechanism used, electrostatic repulsion and steric interaction from adsorbed polymers. The most widely exploited affect of non-ionic polymers on colloidal stability is called steric stabilization, in which stability is imparted by polymer molecules that are adsorbed onto or attached to the surface of the colloid particle. Electrostatic stabilization results from control of the pH by acid or alkali and the ionic strength imparted by the added salt. In electrostatic stabilization, the mechanisms of change formation are surface dissociation and adsorption of ions from the solution. The charged surface reacts as an agent attaching to the colloid particles and changes the original charges. The electrophoretic mobility is proportional to the zeta potential and is thus a qualitative measure of colloid stability. Therefore to find how to prevent aggregation and accelerate dispersion, the variation in suspension behaviour with pH which determines the surface charge and the affect of dispersion on the sintered specimens are the subjects of this study. From these results, enhancement of sintered density and stability from abnormal grain growth may be expected.

## 2. Experimental details

For the sol–gel method, barium acrylate and lead acetate salts were used as the barium and lead sources with purity of 95% and 99%, respectively, and titanium isopropoxide alkoxide was used as the titanium source with a purity of 95%. The alkoxide and salts are extremely moisture prone and carbon dioxide sensitive materials, thus these materials were handled under a nitrogen atmosphere. Barium acrylate was dissolved in dry ethylene glycol and methoxyethanol. Lead acetate was dissolved in dry methoxyethanol and then titanium isopropoxide was mixed in until it dissolved. The solutions were refluxed and dissolved again completely. The solutions were kept at room temperature and at 70° C, respectively. A mixture of these solutions was allowed to dissolve sufficiently, and the hydrolysis was allowed to take place by introducing the alkoxides to excess water under vigorous stirring. Hydrolysis was carried out using a solution of methoxyethanol and double distilled deionized water (1 : 2 ratio) in excess proportion (100 mole of water per mole of alkoxide) [8]. After hydrolysis, the solution was peptized with acrylic acid in the range from 0.007 to 0.024 mole. The gel which formed was then dried. The dispersion behaviour of the prepared fine particles was observed in the suspension as a function of pH. The solution pH was adjusted in the range from pH 1 to 13 using $NH_4OH$ or HCl. The suspension was stirred by magnetic stirrer and a pH meter was used. The $(Ba_{0.2}Pb_{0.8})TiO_3$ powder was allowed to synthesize at 600° C for 1 h. The calcined powders were milled and mixed with 0.5 wt% PVA binder. The powders were then pressed under a pressure of 700 kg $cm^{-2}$ and then isostatically pressed under 1500 kg $cm^{-2}$ into pellets 10 mm in diameter and 3 mm thick.

The specimens were sintered in several high purity alumina crucibles packed with powder of the same composition and industrial $ZrO_2$ powder to maintain



0022–2461/90 $03.00 + .12 

a lead atmosphere. The pellets were fired in air at 500° C for 1 h to eliminate the PVA binder after heating at a rate of 200° C $h^{-1}$ and then sintered at 1200° C for 30 min after heating at a rate of 300° C $h^{-1}$. The rapid heating rate and short soaking time were used to prevent evaporation of the lead. Electrodes were connected to both surfaces of the specimens with high-temperature silver paste by the screen method for electric measurements and heated to 870° C for 10 min. Information for the identification of phases and the molecular structure of the components, especially organic materials, and the degree of reactivity were obtained by means of X-ray diffraction and IR spectrum measurements. The dispersion behaviour was observed by measuring the surface area, zeta potential and viscosity. The sinterability was studied in terms of the density and microstructure. The dielectric constant was calculated from the measured capacitance using an LCR meter.

## 3. Results and discussion

The $H^+$ and $OH^-$ ions are presumably potential-determining ions. At low pH, OH attaches to the surface of the excess protons and the net charge of the surface is positive. At high pH, the protons separate from the surface due to the excess OH and then the net charge is negative due to the loss of protons.

For $(Ba, Pb)TiO_3$, at low pH

$$(Ba_{1-x}Pb_x)Ti(OH)_6 + 6H^+ \rightarrow (Ba_{1-x}Pb_x)Ti(OH)_6 \quad (1)$$

and at high pH

$$(Ba_{1-x}Pb_x)Ti(OH)_6 + 6OH^- \rightarrow (Ba_{1-x}Pb_x)TiO_6^- + 6H_2O \quad (2)$$

A plot of zeta potential against pH for the sol–gel derived $(Ba_{0.2}Pb_{0.8})TiO_3$ gel is given in Fig. 1 to show the colloidal stability. The point of zero charge (p.z.c.) is found to occur at $Ba^{+2}$, $Pb^{+2}$, $Ti^{+4}$ ion concentrations of $2.0 \times 10^{-7}$, $5.01 \times 10^{-7}$, and $1.0 \times 10^{-6}$ M, respectively, or $P_{Ba} = -\log[Ba^{+2}] = 6.7$, $P_{Pb} = -\log[Pb^{+2}] = 6.3$, $P_{Ti} = -\log[Ti^{+4}] = 6.0$. A point of zero charge ($\xi = 0$) with positive and negative charge branches is shown in Fig. 1. The charge simply decreases to zero with an increase in pH up to pH 7 and becomes increasingly negative with an increase in pH. The i.e.p., pH 7, of the $(Ba_{0.2}Pb_{0.8})TiO_3$ is in accordance with the z.c.p. of each ionic solid. TGA curves for the sol–gel derived $(Ba_{0.2}Pb_{0.8})TiO_3$ powders are given in Fig. 2. The drastic weight loss is attributed to dehydration and the loss of volatile organic solvent residue from the solution at high temperature for pH 11 and 13. Mazdiyasni [9] studied the preparation of fine particles and their application for the perovskite materials. In this report a well dispersed colloidal system with good reactivity accelerates the removal of organic residue from the solution and maintains deagglomerative conditions. For a calcium oxalate monohydrate surface at high zeta potential, there is good elimination of organic materials as reported by Currie *et al.* [10] using the Nernst equation. Fig. 3 shows the weight loss of $(Ba_{0.2}Pb_{0.8})TiO_3$ powder as a function of pH. At pH 1, 11 and 13, extreme weight loss is shown due to the well dispersed system, but at i.e.p., pH 7, the weight loss is small. Extensive reviews of the charge-potential behaviour of colloidal systems have been given by Hunter [11] and Healy [12]. The most important dissociable groups are of the strong acid (sulphate, sulphonate), weak acid (sulphite, carboxyl), weak base (amine) and strong base (quaternary ammonium) types and they may occur alone at the surface or in various combinations. These combinations form zwitterionic surfaces and then the driving force removed from the system is replaced by

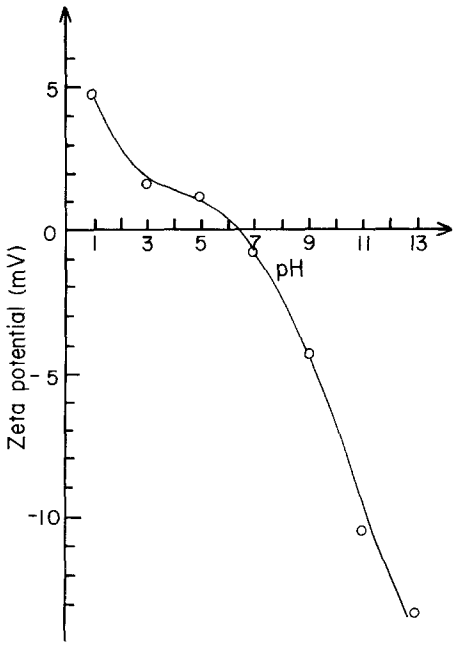


*Figure 1* Zeta potential as a function of pH for the sol–gel derived $(Ba_{0.2}Pb_{0.8})TiO_3$.

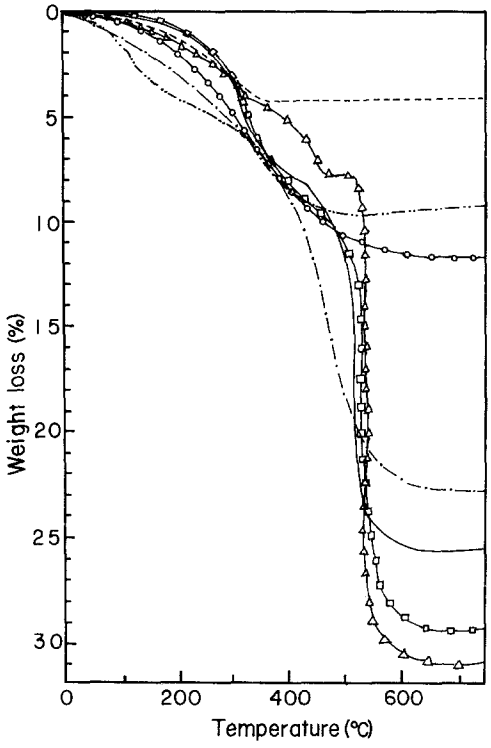


*Figure 2* Thermogravimetry as a function of pH (—— pH 1, –·–·– pH 3, –··–··– pH 5, – – – pH 7, ○ pH 9, □ pH 11, △ pH 13) for the sol–gel derived $(Ba_{0.2}Pb_{0.8})TiO_3$.

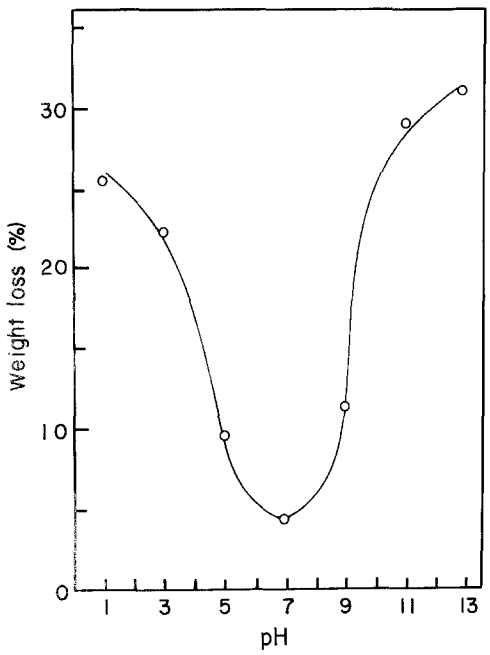


*Figure 3* Weight loss as a function of pH for the sol–gel derived $(Ba_{0.2}Pb_{0.8})TiO_3$.

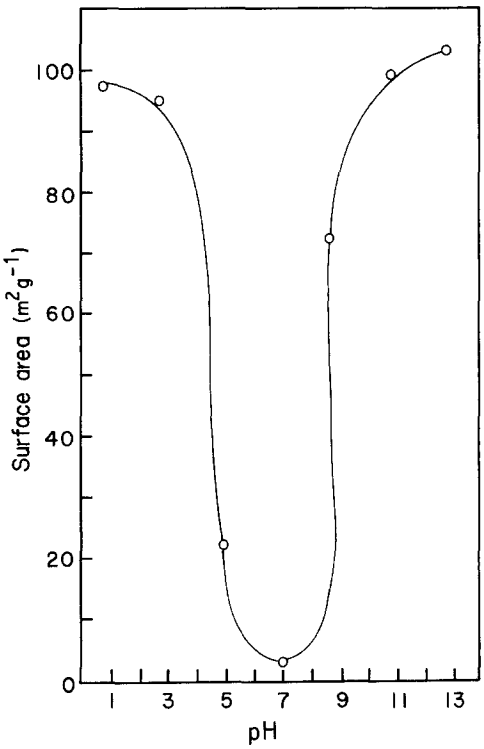


*Figure 4* Surface area as a function of pH for the sol–gel derived $(Ba_{0.2}Pb_{0.8})TiO_3$.

repulsive and interactive forces. Homola and James [13] showed that models of the surface dissociation process are very useful for describing polymer latex systems, which often have carboxyl, sulphate, and sulphonate groups on their surfaces and which can form a zwitterionic surface, and for interpreting the behaviour of oxide surfaces. This tendency is similar to our results. Fig. 4 shows that the specific surface area is dependent on the pH for the sol–gel derived $(Ba_{0.2}Pb_{0.8})TiO_3$ powders.

Electrostatically dispersed suspensions can be realized at pH 11 and 13 as shown in Figs 1 and 2 and they result in a high rate of reactivity and the highest

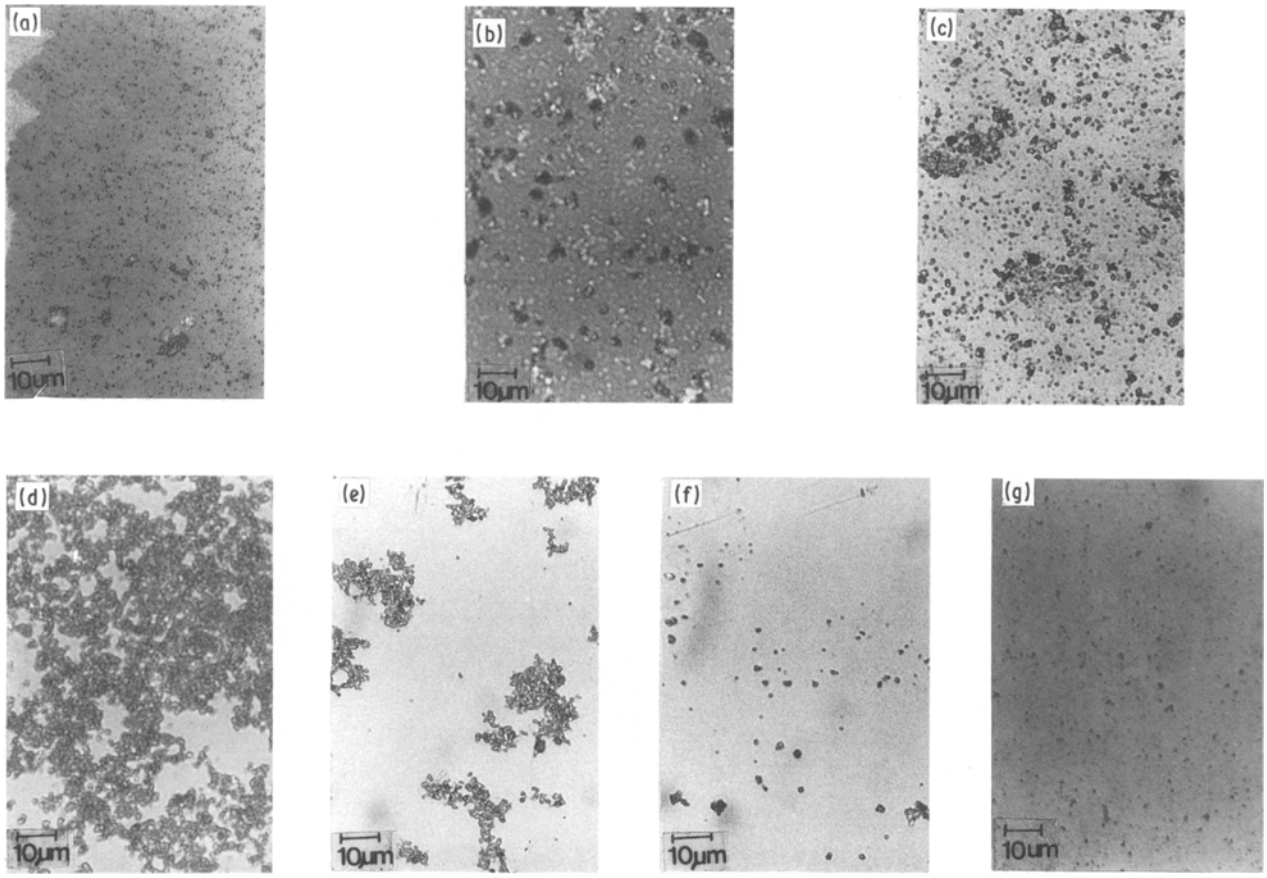


*Figure 5* Metallurgical microscope photographs of the sol–gel derived $(Ba_{0.2}Pb_{0.8})TiO_3$: (a) pH 1, (b) pH 3, (c) pH 5, (d) pH 7, (e) pH 9, (f) pH 11, (g) pH 13 (× 600).

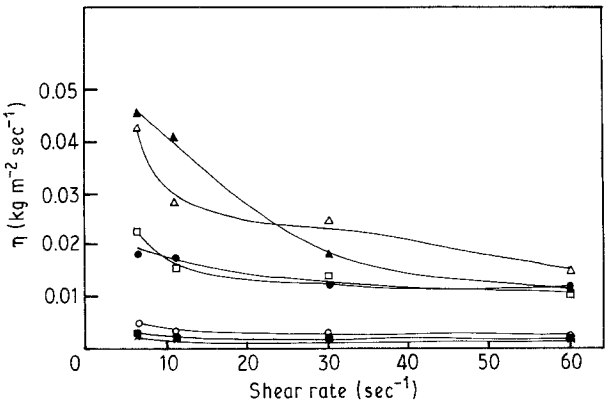


*Figure 6* Suspension viscosity plotted against shear rate for the sol–gel derived $(Ba_{0.2}Pb_{0.8})TiO_3$. (○ pH 1, ● pH 3, △ pH 5, ▲ pH 7, □ pH 9, ■ pH 11, × pH 13).

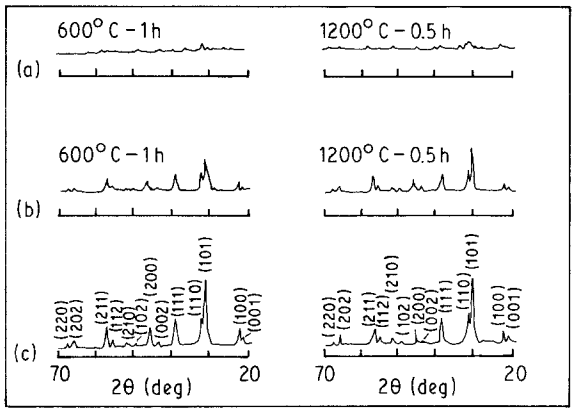


*Figure 7* X-ray diffraction patterns of the sol–gel derived $(Ba_{0.2}Pb_{0.8})TiO_3$. (a) pH 1, (b) pH 7, (c) pH 13.

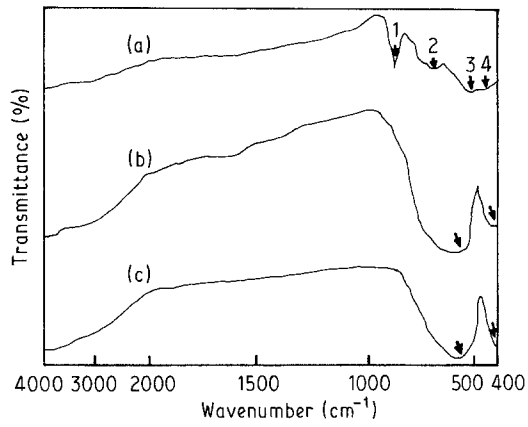


*Figure 9* Infrared transmission of the sol–gel derived and calcined $(Ba_{0.2}Pb_{0.8})TiO_3$: (a) pH 1, (b) pH 7, (c) pH 13.

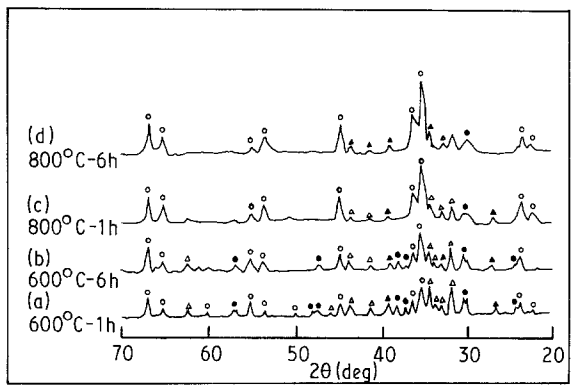


*Figure 10* X-ray diffraction patterns of the sol–gel derived and calcined $(Ba_{0.2}Pb_{0.8})TiO_3$ dispersed in pH 1. (○$(Ba_{0.2}Pb_{0.8})TiO_3$, △ $BaCl_2$, ● $PbTi_3O_7$, ▲ $(Pb_{0.8}Ti_{0.2})Ti_8$).

specific surface area. The measure of surface chemistry of $Pb(Mg_{1/3}Nb_{2/3})O_3$ powders, the zeta potentials, calculated using the Smduchowdki equation as a function of solution pH has been reported by Shrout [14]. Metallurgical microscope photographs of the sol–gel derived $(Ba_{0.2}Pb_{0.8})TiO_3$ with various pH were observed and the results are shown in Fig. 5. As shown in this figure, the case of pH 7 was found to be highly agglomerated and pH 11 and 13 indicate good dispersion. The results correlate with the weight loss and BET values shown in Figs 3 and 4. Fig. 6 shows a plot of viscosity as a function of shear and pH for the sol–gel derived $(Ba_{0.2}Pb_{0.8})TiO_3$ powders. In the samples with pH 3 to 9, the shear thinning phenomenon is apparent, demonstrating that viscosity decreases with increasing shear rate. This phenomenon results from fracture of the soft agglomerate by the high shear and the resulting arrangement of anisotropic particles. X-ray diffraction patterns of the calcined powders and the sintered specimens of the sol–gel derived $(Ba_{0.2}Pb_{0.8})TiO_3$ are shown in Fig. 7. In the pH 1 pattern, not only the characteristic peaks of the solid solution but also second-phase peaks are found. For the pH 13 specimen, however, only the characteristic peaks of the solid solution appear. At low pH, the degree of

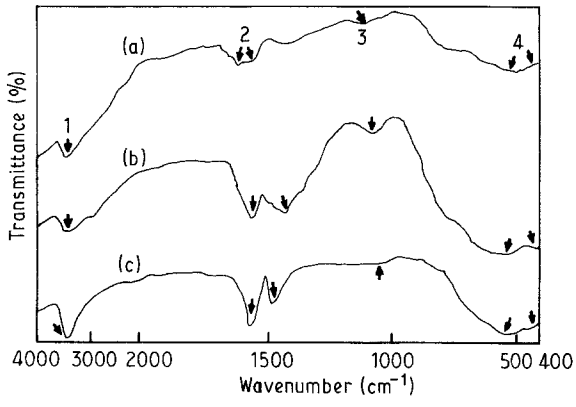


*Figure 8* Infrared transmission of the sol–gel derived $(Ba_{0.2}Pb_{0.8})TiO_3$ gel: (a) pH 1, (b) pH 7, (c) pH 13.

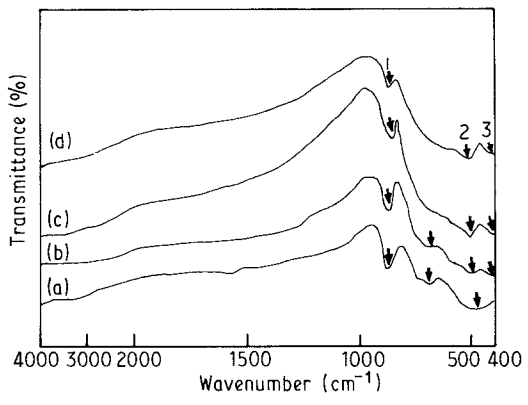


*Figure 11* Infrared transmission of the sol–gel derived and calcined $(Ba_{0.2}Pb_{0.8})TiO_3$ dispersed in pH 1. (a) 600° C, 1 h, (b) 600° C, 6 h, (c) 800° C, 1 h, (d) 800° C, 6 h).

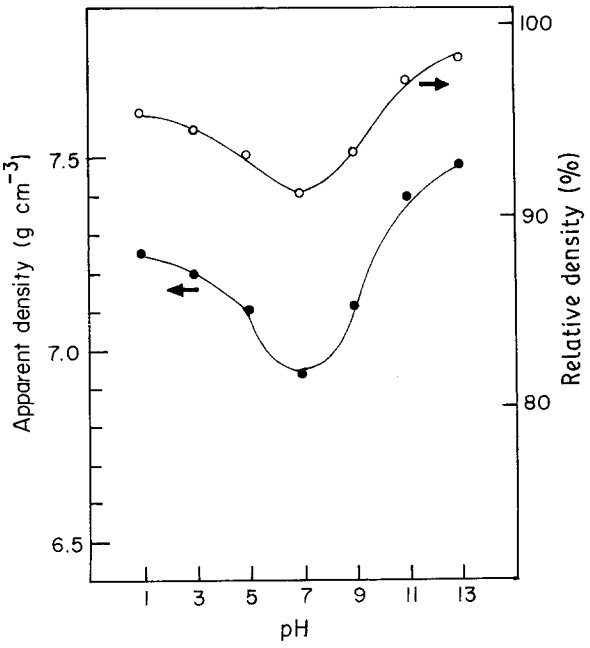


*Figure 12* Apparent and relative density plotted against pH for the sol–gel derived $(Ba_{0.2}Pb_{0.8})TiO_3$ sintered at 1200° C for 0.5 h.

crystallinity reduces and the powder is not synthesized completely. Fig. 8 shows the IR absorption spectra of the sol–gel derived $(Ba_{0.2}Pb_{0.8})TiO_3$ dried gel for various pH. Over the entire range of pH no H–Cl and N–H bonds, which are used to adjust the pH, are found, though the characteristic peaks are found from the raw materials. Fig. 9 shows infrared adsorption spectra of the sol–gel derived $(Ba_{0.2}Pb_{0.8})TiO_3$ calcined powder for various pH. The intensity of the hydrogen bond and the characteristic bond of the organic compound in the dried gel decrease. Peaks 2 and 3 become sharper with increase in pH and shifted to higher frequency as the crystalline phase becomes more stable. At pH 1, there is peak 1, which seems to be the peak of the halogen compound (= 800 cm$^{-1}$; peak 1). The peaks of the $(Ba_{0.2}Pb_{0.8})TiO_3$ solid solution and the unknown second phase are apparent and the degree of crystallization decreases as shown in Fig. 9. To observe the affect of acid the $(Ba_{0.2}Pb_{0.8})TiO_3$ powder was studied to determine if it was synthesized completely at pH 1. X-ray diffraction patterns of the sol–gel derived $(Ba_{0.2}Pb_{0.8})TiO_3$ dispersed in pH 1 under various calcine conditions are shown in Fig. 10. The HCl, which adjusts the pH, extracts barium from the solid solution making $BaCl_2$; this resulted in the formation of $PbTi_3O_7$ and $(Pb_{0.8}Ti_{0.2})Ti_8$. The characteristic peaks of the second phase can not be removed even when the powders are calcined at 800° C for 6 h. Fig. 11 shows the IR absorption spectra of the sol–gel derived $(Ba_{0.2}Pb_{0.8})TiO_3$ dispersed in pH 1 as a function of calcine conditions. The intensity of peak 1 (800 cm$^{-1}$) decreases and the characteristic peaks of (Ba, Pb)$TiO_3$ narrow with increasing calcination time. The sharp peaks suggest an increase in crystallization but not all the unknown peaks disappear. Fig. 12 shows the apparent and relative density for the $(Ba_{0.2}Pb_{0.8})TiO_3$ sintered at 1200° C for 0.5 h as a function of pH. At pH 7 where the dispersion is poor, the density is lower than for other pH. The affect on the sintering mechanism of agglomerate size and particle size in the yttria-stabilized ziroconia has been studied by Rhodes [15]. According to Rhodes' report, an agglomerate with a very open arrangement of crystallites may develop large pores or pore clusters and leave large lenticular voids which are difficult to close. These results decrease the density. Reeve [16] predicted a similar phenomenon in BeO. For the cases of pH 11 and 13, well dispersed systems, the sintered density is high. The densities of pH 1 and 3 leading to the dispersed are higher than that of pH 7 but lower than those of pH 11 and 13. The reason is the densities of $PbTi_3O_7$ and $BaCl_2$ are lower than that of the

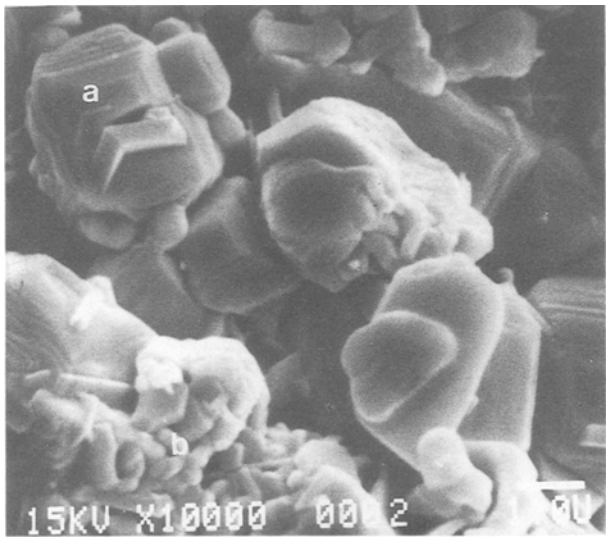


*Figure 13* EDAX analysis of $(Ba_{0.2}Pb_{0.8})TiO_3$ dispersed in pH 1 and sintered at 1200° C for 0.5 h.

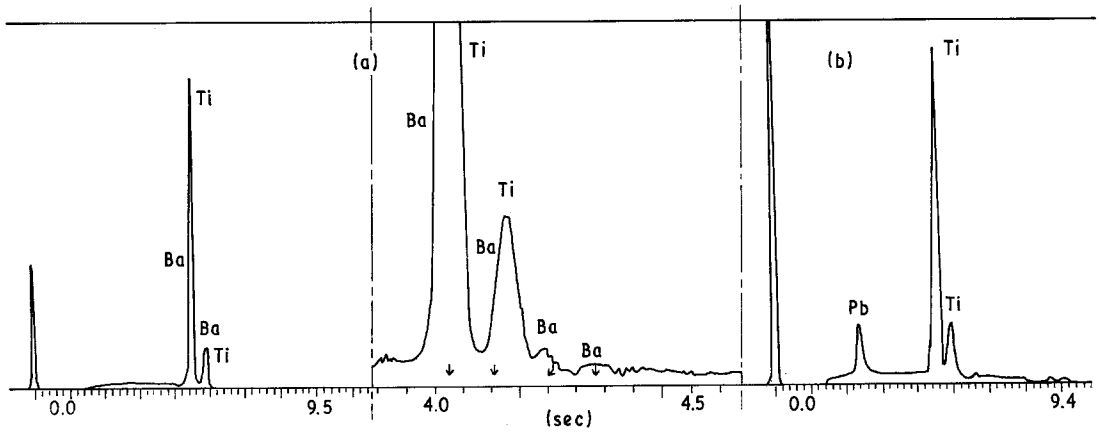

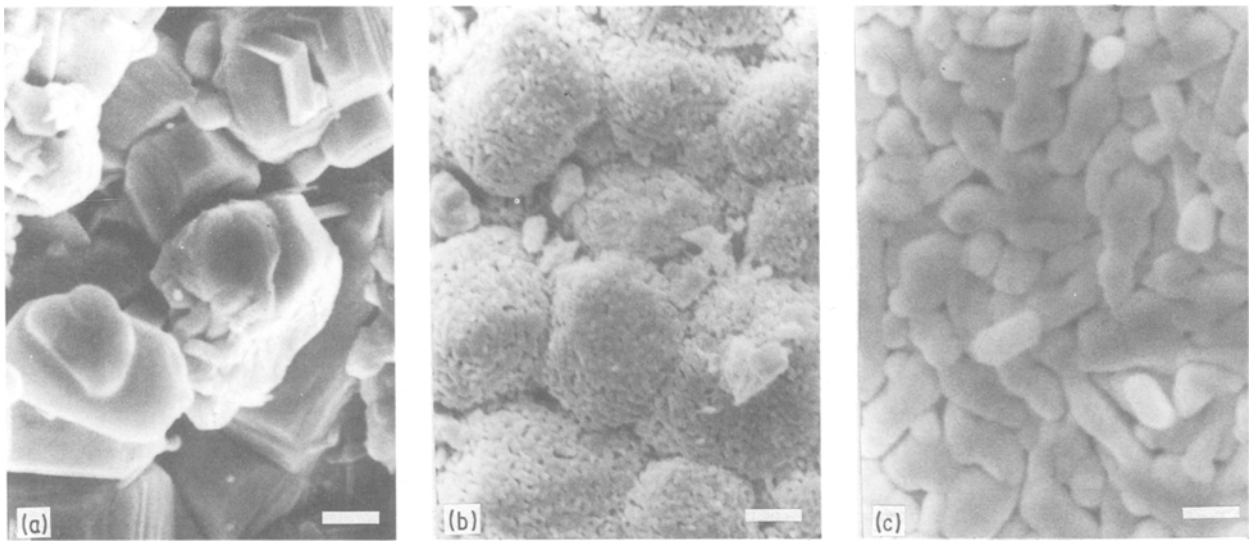


*Figure 14* SEM photographs of $(Ba_{0.2}Pb_{0.8})TiO_3$ sintered at 1200° C for 0.5 h: (a) pH 1, (b) pH 7, (c) pH 13 (bar = 1 $\mu$m).

$(Ba_{0.2}Pb_{0.8})TiO_3$ solid solution. Fig. 13 shows a EDAX analysis of the sol–gel derived $(Ba_{0.2}Pb_{0.8})TiO_3$ dispersed in pH 1 and calcined at 600° C for 1 h and sintered at 1200° C for 0.5 h. In part (a), no lead peak is found and only titanium and barium peaks are found. The eV value of the barium peak is similar to that of the titanium peak, so it is difficult to identify. In part (b) the barium, lead and titanium peaks resulting from the $(Ba_{0.2}Pb_{0.8})TiO_3$ solid solution, $PbTi_3O_7$ and $(Pb_{0.8}Ti_{0.2})Ti_8$ are all identified. According to this EDAX analysis, barium is isolated from the (Ba, Pb)$TiO_3$ solid solution and other phases are formed. SEM photographs of the sol–gel derived $(Ba_{0.2}Pb_{0.8})TiO_3$ as a function of pH are shown in Fig. 14. At pH 13, the grain size is homogeneous while aggregation appears and the sinterability decreases at pH 7. These results back up the density results.

## 4. Conclusions

The conclusions are as follows.

1. The dispersion at pH 7 is an isoelectric point (iep) in the sol–gel derived $(Ba_{0.2}Pb_{0.8})TiO_3$ powder, and better dispersion was found at lower and higher pH than at pH 7.

2. The powder has a BET surface area of 2.3 $m^2 g^{-1}$ at pH 7 and 97 to 105 $m^2 g^{-1}$ at pH 1, 11, and 13 respectively.

3. The sol–gel specimens derived from well dispersed suspensions with pH 11 and 13 show a high relative density (95 to 98%).

## Acknowledgement

This work was supported by the Korea Science and Engineering Foundation.

## References

1. S. SAKKA, *Amer. Ceram. Soc. Bull.* **64** (1985) 1463.
2. D. L. SEGAL, *J. Non-Cryst. Solids* **63** (1984) 183.
3. M. E. A. HERMANS, *Powder Metal Int.* **5** (1973) 137.
4. H. DISLICH and P. HINZ, *J. Non-Cryst. Solids* **48** (1982) 11.
5. K. H. JO and K. H. YOON, *Mater. Res. Bull.* **24** (1989) 1.
6. R. H. ALVAREZ, F. J. NIEVES and G. PARGO, *J. Coll. Int. Sci.* **107** (1985) 77.
7. K. W. LEE, *ibid.* **108** (1985) 109.
8. D. R. OHLMANN, *J. Amer. Ceram. Soc.* **70** (1987) 28.
9. K. S. MAZDIYASNI, *Amer. Ceram. Soc. Bull.* **57** (1978) 448.
10. P. CURRERI, G. Y. ONODA, Jr. and B. FINLAYSON, *J. Coll. Int. Sci.* **69** (1979) 170.
11. R. J. HUNTER, in "Zetapotential in Colloid Science" (Academic Press, New York, 1981) p. 134.
12. T. W. HEALY and L. R. WHITE, *Adv. Coll. Int. Sci.* **9** (1978) 303.
13. A. HOMOLA and R. O. JAMES, *J. Coll. Int. Sci.* **59** (1977) 123.
14. T. R. SHROUT, B. JONES, J. V. BIGGERS and J. H. ADAIR, in "Ceramic Transaction" (American Ceramic Society, Ohio, 1988) p. 519.
15. W. H. RHODES, *J. Amer. Ceram. Soc.* **64** (1981) 19.
16. R. D. REEVE, *Amer. Ceram. Soc. Bull.* **42** (1963) 452.

*Received 6 April*
*and accepted 16 August 1989*